RAPID COMMUNICATIONS

PHYSICAL REVIEW A VOLUME 51, NUMBER 6 JUNE 1995

Interferences in photoexcited double-excitation series of He

M. Domke, K. Schulz, G. Remmers, A. Gutiérrez, and G. Kaindl
Institut für Experimentalphysik, Freie Universität Berlin, Arnimallee 14, D-14195 Berlin-Dahlem, Germany

D. Wintgen
Fakultät für Physik, Universität Freiburg, Hermann-Herder-Straße 3, D-79104 Freiburg, Germany
(Received 11 July 1994)

The double-excitation $^1P^o$ Rydberg series of He, converging to the $N=4$ to 9 thresholds, were studied by high-resolution photoionization using synchrotron radiation. Both the principal series with correlation quantum numbers $K=N-2$ and the secondary series with $K=N-4$ could be resolved up to previously unobtained n values. This allows a substantially improved analysis of the series with respect to energies and linewidths, leading to an improved understanding of the interseries interferences. The data are in excellent agreement with calculations based on the complex-rotation method.

PACS number(s): 32.70.Fw, 32.80.−t, 31.50.+w, 31.25.Jf

Doubly-excited He represents the simplest two-electron atom and is therefore a prototype system for electron correlation studies. There is now a renewed theoretical interest in these excitations [1–5] mainly because of the substantially improved experimental data that recently became available due to advances in resolution and photon flux [6,7]. Highly excited He atoms are often called "planetary atoms" due to their large sizes; they are still not sufficiently well understood, both from a theoretical and an experimental point of view. A large number of double-excitation Rydberg series have been experimentally observed, characterized by the quantum number N of the "inner" electron and consisting of autoionizing Fano resonances with the running quantum number n of the outer electron ($n \geqslant N$). Due to the dipole selection rules, only $^1P^o$ final states can be photoexcited. In general, up to $(2N-1)$ different $^1P^o$ series exist for a given N; they differ by the correlation quantum numbers K, T, and A [8], leading to the nomenclature $N(K,T)_n^A$ or—in short—N,K_n [9]. The main series are characterized by $T=1$, $A=+$, and $K=N-2,N-4,\ldots,-(N-2)$, i.e., $N(K,1)_n^+$. Most intense is the principal series with $T=1$ and maximum K, i.e., $K=N-2$, where the two electrons reside predominantly on opposite sides of the nucleus. The other possible series have strongly decreasing transition probabilities in the order $K=N-4$, $K=N-6,\ldots$, which is the reason why only a few lines of these series could be observed up to now. The $T=0$ series with K ranging from $N-1$ to $-(N-1)$ are much weaker and have only been observed up to now for $N=2$ in the form of the $2,1_n$ and $2,-1_n$ series [7], which have also been designated as $(sp,2n-)$ and $(2p,nd)$ series, respectively.

For low-N values, the resonances experience only the interaction of the doubly-excited He atom with one continuum ($\cong N-1$), giving rise to simple Fano profiles of the excitation cross section. An additional decay channel appears for higher N values ($N \geqslant 5$), where the energies of the high-n resonances of the N series overlap with the lowest member(s) of the $(N+1)$ series. This leads to interseries interferences with anomalies in peak height, linewidth, and quantum defect. The lowest interferences $5,3_n/6,4_6$ and $6,4_n/7,5_7$ have been experimentally identified recently [6], but resonances with $N \geqslant 7$ have not been reported up to now, mainly because of their very low intensities. On the other hand, these high-N series are crucial for an improved insight into electron correlation in this prototype three-body system.

In the present Rapid Communication, we report on experimental results of double-excitation resonances of He in the $N=7$ to 9 region, including several interseries interferences between high-n resonances of series N with the first and second members of series $(N+1)$. We have also identified secondary series with $K=N-4$. In addition, considerably improved double-excitation spectra for $N=4$ to 6 are presented. The experimental resonance parameters (energies, linewidths, line forms, quantum defects) are compared in detail with theoretical results obtained by the complex-rotation method.

The measurements were performed with the high-resolution plane-grating monochromator SX700/II of the Freie Universität Berlin at the Berliner Elektronenspeicherring für Synchrotronstrahlung (BESSY) [10], using a 2442-lines/mm grating in small-source operation of the electron storage ring. The resolution ΔE at a photon energy of 65 eV was then 4.1 meV (full width at half maximum) [7]; it extrapolates to $\Delta E \cong 5.4$ meV at $h\nu=78$ eV, using the relation $\Delta E \propto E^{3/2}$ [10]. Photon energies were calibrated by measuring the $2,1_3$ resonance at 62.758 eV [7] [$(sp,23-)$ in the nomenclature of Refs. [6,7]]; the theoretical energies were adjusted to this line using a double-ionization potential $I(\mathrm{He}^{2+})=79.0030$ eV and $R_{\mathrm{He}}=13.603\,83$ eV. Photoabsorption spectra were taken by recording the photoionization current as a function of photon energy with an ionization chamber of 10-cm active length filled with He at pressures of 1 to 3 mbar. The chamber was separated from the ultra-high-vacuum monochromator by a 1200-Å-thick carbon window.

Theoretical calculations of resonance parameters and cross sections were performed with the complex-rotation method, as described in Ref. [4]. We extended those calculations up to the $N=9$ threshold and checked convergence of our results by systematically increasing the set of basis functions. Resonance parameters (widths and positions) were typically converged to eight significant digits. For isolated

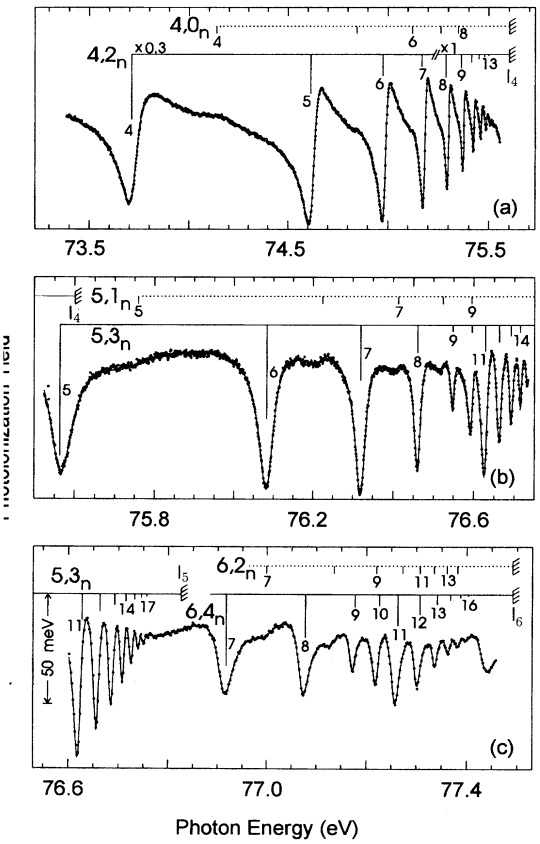

FIG. 1. Double-excitation spectra of He below the $N=4$, 5, and 6 thresholds: (a) the almost undisturbed $N=4$ series, (b) the $N=5$ series, and (c) the $N=6$ series interfering with the $6,4_6$ and $7,5_7$ resonances, respectively. The solid lines through the data points represent the results of least-squares fits. Note that the photon-energy scales are expanded by factors of 2 and 2.5 in the cases of spectra (b) and (c), respectively. The vertical-bar diagrams give the energies of resonances as obtained from complex-rotation calculations adjusted to the $4,2_6$ resonance. The lengths of the vertical bars represent *calculated* linewidths in case of the principal series, $N,(N-2)_n$ (solid bars), with the same linewidth scale in all bar diagrams [except for a factor of 0.3 in part of (a), as indicated]. For the secondary series (dotted bar diagrams) $N,(N-4)_n$, only energies are given.

resonances, i.e., in cases where contributions of different states did not overlap, we found good agreement between calculated and measured Fano-shape parameters. We typically found that the transition strengths (intensities in the experimental spectra) and the linewidths of the resonances were strongly correlated and approximately proportional to each other. Such a behavior reflects the propensity rules for the decay of the resonances as discussed for $^1S^e$ states [11].

In Fig. 1, photoionization spectra are presented in the regions of (a) the $N=4$ Rydberg series (almost undisturbed), and (b) and (c) the strongly disturbed $N=5$ and $N=6$ series. For all three series, the results of our calculations concerning energy positions and linewidths are given in the form of bar diagrams; in the case of the principal $N,(N-2)_n$ series, the lengths of the vertical bars represent the calculated linewidths. The resonance lines in the $N=4$ series exhibit steadily decreasing peak heights expected from a convolution of the monochromator function with the resonances of width Γ; Γ depends on n according to $\Gamma_n \propto (n-\delta_n)^{-3} = n^{*-3}$ (δ_n is the quantum defect; n^* is the effective quantum number). On the other hand, the $N=5$ ($N=6$) series exhibit strong interseries interferences around $h\nu = 76.6$ eV (77.2 eV), with a resonancelike variation of the peak heights, caused by an interaction of the broad $6,4_6$ ($7,5_7$) resonance with the narrow $5,3_n$ ($6,4_n$) lines. Compared to previous measurements [6], both the resolution and the statistical accuracy of the data have been considerably improved, and the Rydberg series could be resolved up to much higher n values than before, i.e., to $n=17$ for the $5,3_n$ series and to $n=16$ for $6,4_n$. This provides much more reliable results on the parameters describing the resonances (like energy E_r, linewidth Γ, quantum defect δ, and Fano parameter q). The cross sections of the individual resonance lines were derived by fitting independent Fano profiles [12] to the lines, given by $\sigma = \sigma_a (q+\varepsilon)^2/(1+\varepsilon^2) + \sigma_b$, with $\varepsilon = 2(E-E_r)/\Gamma$ and σ_a assumed to be approximately constant within one series. A comparison with the theoretical linewidths Γ_n (see bar diagrams) shows that the anomalous resonancelike variations in peak height are to a large extent caused by these variations in linewidth.

The $4,2_n$ series [Fig. 1(a)] is not undisturbed, since its highest members overlap with the $5,3_5$ resonance at $\cong 75.56$ eV. This actually prevents the observation of lines with $n>14$, which should be well resolved, if a constant reduced linewidth $\Gamma_n^* = \Gamma_n n^{*3}$ is assumed. In the interference regions of the $5,3_n$ and $6,4_n$ series, the linewidths (and hence also the line intensities) show strong deviations from the simple monotonic behavior. In fact, the linewidth decreases anomalously strongly from $n=8$ to 9 and increases in a resonancelike manner when proceeding to $n=11$, i.e., it reveals overall a Fano-like dependence (see below). There is also a change of the Fano q parameter in the interference region. In contrast to former results [6], however, the strongly improved spectra reveal that q is not typically changing sign ("Fano-q reversal"), but is instead increasing from $q \cong -0.3$ to values close to zero in the interference region.

In addition to the principal Rydberg series $(4,2_n;5,3_n;6,4_n)$, the first members of three other Rydberg series can be recognized in the spectra of Figs. 1(a)–1(c); we assign them to the secondary Rydberg series $4,0_n;5,1_n;6,2_n$. Note that the higher members of these secondary series overlap with resonance lines of the respective principal series. These overlaps limit to some extent the reliability of some of the parameters derived for the principal series, particularly of the Fano-q parameters. They have no influence, however, on the general trends discussed in the present work.

The secondary series $4,0_n;5,1_n;6,2_n$ have some noteworthy properties. (i) The resonance lines are broader than those of the neighboring principal series, which is opposite to observations for the secondary series $2,1_n$, $2,-1_n$ and the $3,-1_3$ resonance; these were found to be narrower than the respective neighboring principal resonances [6,7]. (ii) Only the $4,0_n$ Rydberg series has a "positive" line shape ($q>1$). For $N>4$ the Fano parameters decrease to $q<1$ for the sec-

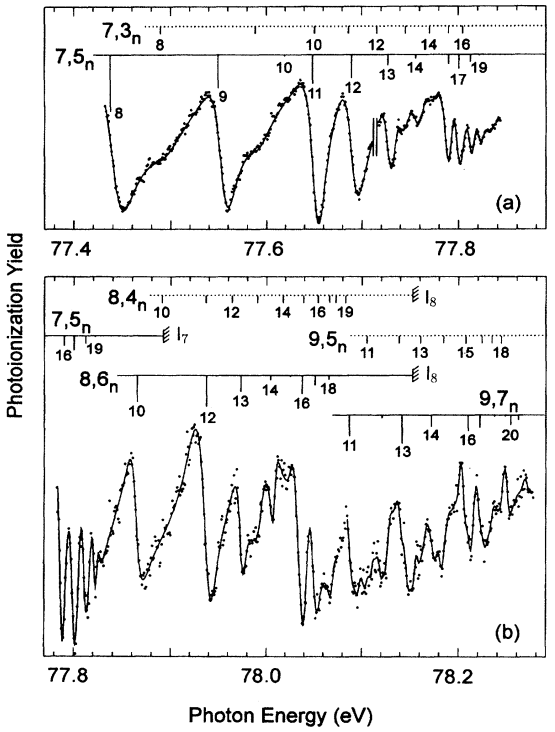

FIG. 2. Double-excitation spectra of He below the $N=7$ to 9 thresholds: (a) The $7,5_n$ and $7,3_n$ series, with the $7,5_n/8,6_8$ and the $7,5_n/8,6_9$ interseries interference regions. The left part of the spectrum (up to 77.71 eV) was taken with a slightly worse resolution ($\Delta E \cong 8$ meV). (b) The $8,6_n$ and $9,7_n$ principal series as well as the $8,4_n$ and $9,5_n$ secondary series. The solid curves through the data points represent the results of least-squares fits; for $h\nu \geq 78.08$ eV, the solid curves serve as a guide to the eye. The bar diagrams have the same meaning as in Fig. 1: the vertical bars represent *calculated* energies and linewidths (the latter only for the $7,5_n$;$8,6_n$;$9,7_n$ series).

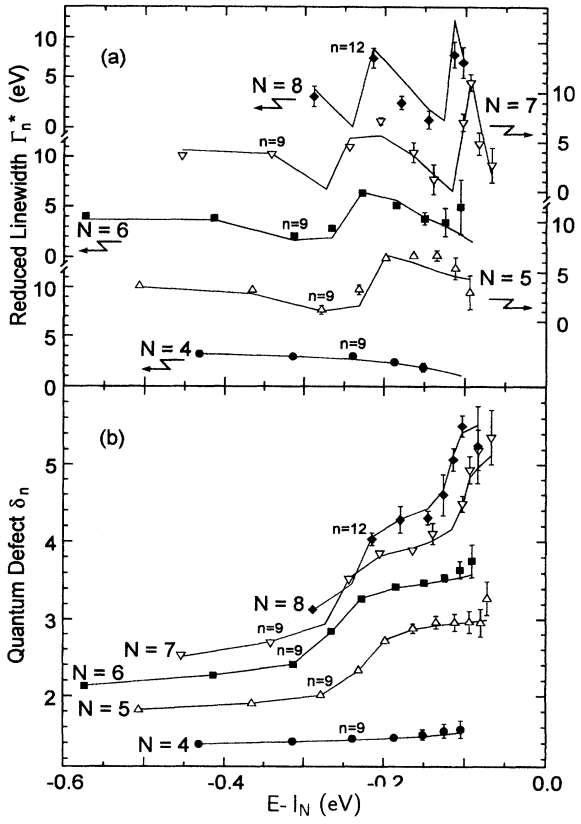

FIG. 3. Experimental results for the principal series $N=4$ to 8: (a) reduced linewidth $\Gamma_n^* = \Gamma_n n^{*3}$; (b) quantum defect δ_n, both as a function of the energy difference to the relevant threshold I_N, taken from theory. N is the quantum number of the inner electron. The solid lines connect the theoretical results for different n. For clarity, the ordinate scale in (a) is shifted by 6.5 eV between neighboring N values. Note the Fano-like variation of Γ_n^* and the arctan-like increases of δ_n by "1" in the interference regions, as well as the gradual increase of δ_n with n outside of interference regions, becoming steeper for higher N values.

ondary series $5,1_n$, $6,2_n$, and $7,3_n$ describing "negative" line shapes as in the case of the principal series with $N \geq 4$ [1,2,4,6,7]; these "negative" line shapes are also called window resonances. This finding is in agreement with the results of our complex-rotation calculations, but disagrees with previous high-noise measurements [9].

In Fig. 2(a), the $N=7$ double-excitation Rydberg series are shown; here *two* resonances of the next principal series, $8,6_8$ and $8,6_9$, are obviously interfering with the $7,5_n$ series in the regions of the $n=10,\ldots,14$ and $15,\ldots,18$ resonances, respectively. More importantly, interference effects are much more dramatic than for $N=5,6$. Interference patterns similar to $N=5,6$ are observable for n around 17. However, intensity modulations and variations of the linewidths are extremely pronounced in the interference regions $n=9,\ldots,12$ and $14,\ldots,16$. The $7,5_{10}$ and $7,5_{15}$ resonances are even fully suppressed in the cross section and their widths are anomalously small. This points to a really Fano-like dependence of Γ_n^*, as shown in Fig. 3(a). In the case of the $N=7$ series, the minimum in Γ_n^* is found at *integer* n values, which is not the case for the $N=5$ and 6 series. In particular, we point out the following observations. (i) The $7,5_{10}$ and $7,5_{15}$ resonances are missing in the spectrum of Fig. 2(a), which agrees well with theory. The latter predicts linewidths of $\Gamma_{10}=0.66$ meV and $\Gamma_{15}=0.05$ meV, which amount to only $\cong 3-4$ % of the linewidths of Γ_9 and Γ_{14}, whereas for the $N=5$ and 6 series, the $n=9$ and 10 resonances have linewidths amounting to $\cong 25\%$ of that of the $n=8$ resonance. (ii) The resonances $7,3_8$, $7,3_9$, $7,3_{13}$, and $7,3_{14}$ from the secondary $K=3$ series are clearly visible in the spectra. The other resonances of the secondary series, however, are very close to resonances of the principal series, preventing further insights into interferences within the *secondary* series. (iii) For the principal series, the experimental intensities and the calculated linewidths are closely related, with only minor deviations that can be explained on the basis of overlapping secondary resonances.

Similar effects are observed for the $(9,7_9;9,7_{10})/8,6_n$ interaction regions in the spectrum of Fig. 2(b) around $h\nu \cong 77.92$ and 78.02 eV, respectively. Here, the statistical accuracy of the data gets worse, since the signal intensities are less than 0.001 of the background intensity. Nevertheless,

we can identify interference effects within the $8,6_n$ series by structures in the region $n=12,\ldots,14$ and $16,\ldots,19$, similar to those observed for $7,5_{n=11,\ldots,14}$ and $7,5_{n=16,\ldots,20}$, respectively, as well as by the practically missing $8,6_{11}$ and $8,6_{15}$ resonances. We can also identify a few secondary resonances, in particular, $8,4_{10}$, $8,4_{12}$, and $8,4_{13}$. In case of the $9,7_n$ series, which interacts with the $10,8_{10}$ and $10,8_{11}$ resonances at energies around 78.12 and 78.19 eV, respectively, an unambiguous fit is no longer possible, and assignments become increasingly difficult. They are only feasible by relying on line positions from the calculations, which anyway describe the experimental data rather well.

In Fig. 3, the effects of interference on reduced linewidths Γ_n^* and on quantum defects δ_n, obtained from the analysis of the present spectra, are plotted as a function of $E-I_N$ for the $N=4$ to 8 series. The solid lines connect the *calculated* Γ_n^* and δ_n values, respectively; the points with different symbols for the various N are the fitted *experimental* results. There is a very good agreement of the calculated values with the experimental results, in particular for the δ_n values. The experimental linewidths are sometimes influenced by nearby secondary resonances that cannot be resolved from the principal resonances (see, e.g., the $7,5_{12}$ resonance at -0.2 eV); this leads to slightly larger deviations between theory and experiment. Nevertheless, the effects of the resonances are clearly visible, i.e., the Fano-like variation of the reduced linewidth Γ_n^*, as well as a steep arctanlike increase of the quantum defect δ_n by "1" [13], which defines the positions and the widths of the perturbed state. In the $N=7$ and 8 series, the two interferences are observed by two consecutive Γ_n^* variations and by two arctanlike δ_n increases. In addition, the $N=4$ series shows a preinterference behavior, which is given by a beginning decrease in Γ_n^* and a beginning increase in δ_n. Note also that δ_n increases gradually with n in the noninterference region for all series, which is probably due to the polarizability of the excited He atom; it increases with N as well due to the growing size of the atom.

In conclusion, the experimental data are in excellent agreement with calculations based on the complex-rotation method. This demonstrates the level of sophistication reached in the theoretical description of electron correlation in a prototype three-body system like He.

The work in Berlin was supported by the Bundesminister für Forschung und Technologie, Project No. 05-5KEAXI3/TP03; the work in Freiburg by the Sfb-276 of the Deutsche Forschungsgemeinschaft. We are grateful to D. Delande for providing a Lanczos package for the theoretical calculations as well as to the staff of BESSY for expert assistance.

[1] Y. K. Ho, Z. Phys. D **21**, 191 (1991).
[2] I. Sanchez and F. Martin, Phys. Rev. A **44**, 7318 (1991).
[3] J.-Z. Tang, S. Watanabe, M. Matsuzawa, and C. D. Lin, Phys. Rev. Lett. **69**, 1633 (1992).
[4] D. Wintgen and D. Delande, J. Phys. B **26**, L399 (1993).
[5] F. Martin, Phys. Rev. A **48**, 331 (1993).
[6] M. Domke, C. Xue A. Puschmann, T. Mandel, E. Hudson, D. A. Shirley, G. Kaindl, C. H. Greene, H. R. Sadeghpour, and H. Petersen, Phys. Rev. Lett. **66**, 1306 (1991).
[7] M. Domke, G. Remmers, and G. Kaindl, Phys. Rev. Lett. **69**, 1171 (1992).
[8] C. D. Lin, Phys. Rev. A **29**, 1019 (1984).
[9] M. Zubek, G. C. King, P. M. Rutter, and F. H. Read, J. Phys. B **22**, 3411 (1989).
[10] M. Domke, T. Mandel, A. Puschmann, C. Xue, D. A. Shirley, G. Kaindl, H. Petersen, and P. Kuske, Rev. Sci. Instrum. **63**, 80 (1992).
[11] A. Bürgers and D. Wintgen, J. Phys. B **27**, L131 (1994).
[12] U. Fano, Phys. Rev. **124**, 1866 (1961).
[13] M. J. Seaton, Proc. Phys. Soc. London **88**, 815 (1966).